ISSN 0208-7774 TRIBOLOGIA 5/2018 p. 123–131

Filip WASILCZUK[*], Michał WASILCZUK[**], Michał WODTKE[**]

HYDROSTATIC THRUST BEARING WITH REDUCED POWER LOSSES

WZDŁUŻNE ŁOŻYSKO HYDROSTATYCZNE O ZMNIEJSZONYCH OPORACH RUCHU

Key words: hydrostatic thrust bearing, friction losses, hydrodynamic thrust bearing, hydrostatic pocket size.

Abstract In many cases in rotating machinery, axial load is carried by tilting pad thrust bearings which have been developed since the beginning of 20th century. For high reliability and simplicity, most commonly the bearings are bath lubricated. In the times of sustainable development, however, minimization of friction losses becomes an important criterion for machinery assessment, and a strategic goal of their development. Performed calculations, based on elementary rules of fluid dynamics, showed that shearing losses in specially designed hydrostatic bearings can be considerably smaller than the losses in tilting pad hydrodynamic bearings. The aim of the research described in this paper was to check if the preliminary results presented earlier and conclusions of benefits of the further increase of the size of the hydrostatic pocket can be confirmed with the use of CFD calculations.

Słowa kluczowe: hydrostatyczne łożysko wzdłużne, straty tarcia, hydrodynamiczne łożysko wzdłużne, rozmiar komory hydrostatycznej.

Streszczenie W wielu maszynach wirnikowych obciążenia osiowe są przenoszone za pomocą rozwijanych od ponad 100 lat hydrodynamicznych łożysk wzdłużnych z wahliwymi segmentami. Dla prostoty konstrukcji i dużej niezawodności smarowanie tych łożysk najczęściej jest smarowaniem zanurzeniowym. Jednak w czasach zwiększonej presji na oszczędności energetyczne ograniczanie strat tarcia stało się strategicznym celem rozwoju maszyn. Obliczenia wskazują, że w specjalnie zaprojektowanym łożysku hydrostatycznym można uzyskać znaczące ograniczenia strat tarcia w porównaniu z łożyskiem hydrodynamicznym. Obiecujące wyniki i wnioski z poprzedniej pracy skłoniły autorów do przeprowadzenia obliczeń strat tarcia w łożysku hydrostatycznym za pomocą CFD (Obliczeniowej Dynamiki Płynów) z założeniem dalszego zwiększania rozmiaru komory hydrostatycznej w łożysku, co powinno przyczynić się do dalszej minimalizacji strat tarcia.

INTRODUCTION

Tilting pad bearings used in vertical shaft hydrogenerators are working in hydrodynamic mode of operation with hydrostatic jacking high pressure oil systems used only temporarily in transient states of start-ups and shutdowns. The hydrostatic pockets (recesses, caverns) machined in the sliding surface of the pads tend to be designed as small and shallow, so as not to disturb hydrodynamic pressure generation [**L. 1**]. In rare cases, permanent hydrostatic operation is considered as a simple solution to the problems in thrust bearing operation, as pointed out by Abramovitz [**L. 2**]. In a series of papers, Wasilczuk, et al. described the results of field tests of thrust bearings in pump turbines of one of the Polish power plants. The tests showed the benefits of increasing time of the hydrostatic operation during start-ups and stops [**L. 3**]. Moreover,

[*] The Szewalski Institute of Fluid-Flow Machinery, ul. Fiszera 14, 80-231 Gdańsk, Poland, Environmental Doctoral Study, Gdańsk University of Technology, Faculty of Mechanical Engineering, ul. Narutowicza 11/12, 80-233 Gdańsk, Poland, e-mail: filip.wasilczuk@imp.gda.pl.

[**] Gdańsk University of Technology, Faculty of Mechanical Engineering, ul. Narutowicza 11/12, 80-233 Gdańsk, Poland, e-mail: mwasilcz@pg.edu.pl, e-mail: mwodtke@pg.edu.pl.

the operation of tilting pad thrust bearing in hybrid mode, i.e. with operation of hydrostatic lift system also in the steady state, was tested showing considerably lower temperatures [**L. 4**]. Such atypical mode of operation of a thrust bearing was studied theoretically by Ettles et al. [**L. 5**], who demonstrated thicker films and lower temperature in a bearing with hybrid operation. But the analysis of Ettles results described in [**L. 6**] showed that, contrary to expectations and despite of thicker film, a bearing in hybrid operation had higher friction losses. That was caused by lower temperature and higher oil viscosity. On the other hand, thick film and low temperature are the factors increasing bearing reliability. It can be pointed out that a hydrodynamic bearing used as a hybrid bearing is far from optimum from the point of view of minimizing losses. A stationary hydrostatic bearing with minimum energy consumption should have a larger recess, according to theoretical calculations [**L. 6**], in a stationary hydrostatic pad, and the size of the pocket should be 60% of the pad width. In such a bearing, energy consumption, including the sum of energy consumed for generation of high pressure and the generation of the required oil flow reaches its minimum. Following this result, the authors studied a potential of loss decrease comparing the literature results of calculations of a small size tilting pad thrust bearing and a hydrostatic bearing, identical in terms of size and the number of pads with a cavern of the stationary optimum size of 60%, according to [**L. 7**]. The results shown in **Fig. 1** [**L. 8**] did not confirm expected benefits: At 2000 rpm, the losses are equal for both hydrostatic (HS) and hydrodynamic (HD) bearings, while at 4000 rpm, bearing losses are larger by approximately 20% in the hydrostatic berings. By comparing the components of losses in a hydrostatic bearing, it can be concluded that pumping losses are much lower than film losses, caused by shearing.

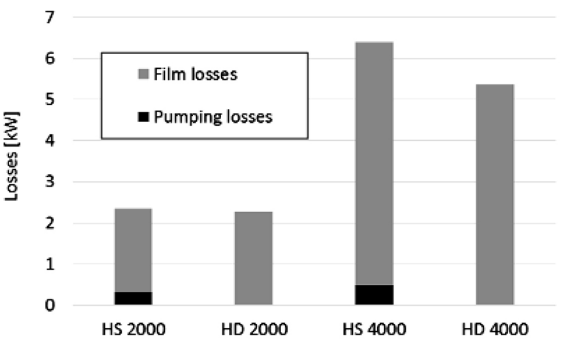

Fig. 1. Losses in both types of bearings: hydrostatic (HS) and hydrodynamic (HD) at 2000 rpm and 4000 rpm [L. 8]

Rys. 1. Straty w łożysku hydrostatycznym (HS) i hydrodynamicznym (HD) przy prędkości obrotowej 2000 obr./min i 4000 obr./min [**L. 8**]

The layout of the bearing studied in that paper is shown in **Fig. 2**, where a deep square-shaped recess with rounded edges can be observed.

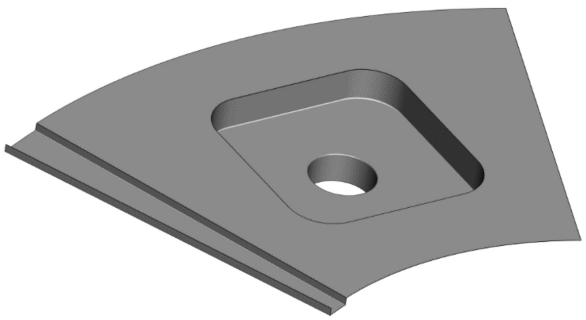

Fig. 2. Hydrostatic bearing layout

Rys. 2. Schemat konstrukcji łożyska hydrostatycznego

Since high shearing rates occur mainly at the surfaces outside the recess, where film thickness is small, it is natural that size of these surfaces should be minimized. This will simultaneously result in an increase of pumping losses, because a narrower thin film area will generate smaller resistance to oil flow and thus increase its amount. However, as this component was much smaller in earlier results (see **Fig. 1**), introducing a bearing with a larger pocket and with narrower edges is hoped to result in a decrease in overall loss, despite the increase of the pumping loss.

GOAL OF THE ANALYSIS

The goal of the analysis was to investigate the impact of the pocket size on the operating parameters of the hydrostatic bearing, focusing on energy saving, because the discussed above increasing the size of the recess should result in an increase of pumping loss and a decrease of shearing loss, generated at the area beyond the pocket. The increase of the pocket size will be continued until a large increase of the pumping loss is observed in the results. The study is a follow-up of a previous investigation that compared the hydrostatic and hydrodynamic bearings operating under the same conditions.

CALCULATION/MODELS

Geometry and calculation models description

The calculations of the hydrostatic bearings were performed in Ansys/Fluent code, by the means of steady RANS simulations. The grid was structured with around 2x106 elements. The schematics of boundary conditions are presented in **Fig. 3**. Four recess sizes were used in simulations for two rotational velocities 2000 rpm and 4000 rpm (**Fig. 4**).

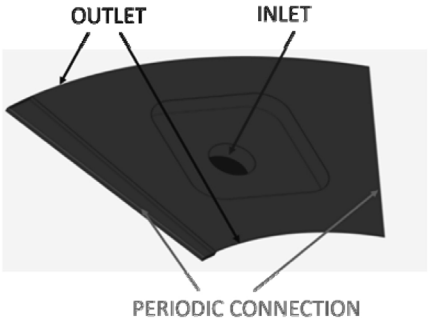

Fig. 3. Hydrostatic bearing boundary conditions schematics
Rys. 3. Schemat warunków brzegowych w łożysku hydrostatycznym

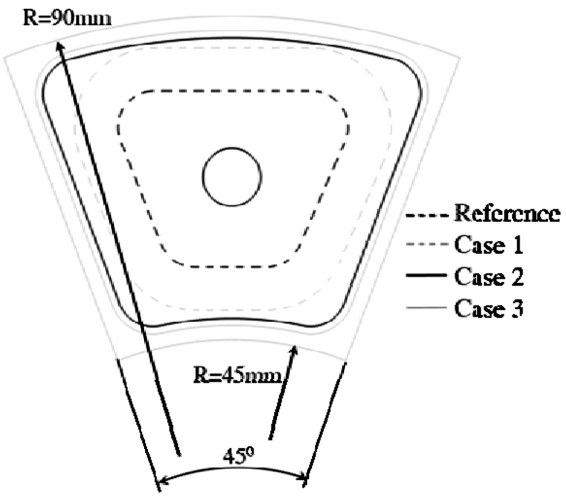

Fig. 4. Four cases of recess size used in calculations
Rys. 4. Cztery przypadki rozmiaru komory wykorzystane w obliczeniach

Film thickness in hydrostatic bearings was assumed constant and equal to that in previous study, i.e. 30.05 μm for 2000 rpm and 37.4 μm for 4000 rpm. The load was 48.3 kN (per 8 segments), and the solution was obtained for two collar rotational speeds – 2000 and 4000 rpm. Finally, ISO-VG 32 oil is used for CFD calculations. Its parameters are presented in **Table 1**. Oil flow is assumed to be incompressible, one-phase, with no cavitation. Oil viscosity varies exponentially with temperature, based on experimental measurements.

Table 1. Parameters of ISO-VG 32 oil
Tabela 1 Właściwości oleju ISO-VG 32

Parameter		Unit	Value
Density	P	[kg/m^3]	856
Specific heat	C	[J/kg K]	2113.5
Viscosity at 40°C	η_{40}	[Pa s]	27.3×10^{-3}
Viscosity at 100°C	η_{100}	[Pa s]	5×10^{-3}

Boundary conditions

Hydrostatic bearing numerical solution was obtained using a pressure based solver using RANS approach with k – ω SST [**L. 9**] turbulence model.

Figure 3 presents the boundary conditions used in the model. At the inlet, constant static pressure was set in addition to oil temperature and turbulence parameters (**Table 2**). The outlet was situated at the inner and outer radii of the film gap with atmospheric conditions. The collar has been assigned appropriate rotational velocity according to the case. Both the collar and the pad walls were adiabatic walls, which are not entirely accurate, but this gives more conservative results when it comes to the film temperatures and loads carried. In order to reduce the computation cost, model features just one of eight pads, thus the rotational periodicity boundary conditions were set.

Table 2. Inlet boundary conditions for hydrostatic bearing model
Tabela 2. Warunki brzegowe na wlocie do łożyska hydrostatycznego

Boundary condition	Unit	Value
Inlet pressure	[MPa]	3.1-5.0
Inlet temperature	[°C]	40
Inlet k	[m^2/s^2]	0.00184
Inlet ω	[1/s]	2.46

The previous study was performed on the model with square-shaped pocket. Increasing the size of the square-shaped pocket would be impractical, since the distance from the edges of the pad would vary significantly for different radii. Therefore, the square pocket was substituted with trapezium (with rounded corners) pocket with the same area, with edges parallel to the edges of the pad. In the 2000 rpm case, this substitution does not impact the losses; however, for the 4000 rpm case, the losses are decreased by 7% for the trapezium pocket. This is a result of highly non-uniform shear stresses on the pad, which are impacted by the shape of the pocket. For the two cases with the largest pocket area, the peripheral edges of the pocket are formed as an arc of the circle. The pocket sizes with respect to pad area were 26% (reference), 60% (6 mm offset from the reference), 70% (walls of the pocket located 3 mm from the pad edges), and 80% (walls of the pocket located 2 mm from the pad edges), as presented in **Fig. 4**.

RESULTS

Main operational parameters

The aim of the paper is to investigate what is the impact of the size of the pocket on the operational parameters

of the hydrostatic bearing. This impact is similar in nature for both rotational velocities; however, it is more visible for 4000 rpm rotational velocity. Oil pressure, temperature, and shearing stress for reference, Case 1 and Case 3, are shown in **Fig. 5** (2000 rpm) and **Fig. 6** (4000 rpm).

With the increase of the pocket size, the feeding pressure decreases. Almost uniform pressure is present in the pocket, equal to the feeding pressure, while outside of the recess, it decreases linearly, accordingly to the theory for pressure losses in a parallel gap. The gradient of the drop increases with increasing the pocket. Both the average and the maximum temperatures in the film decreases with the increase of the pocket, since more cold oil is introduced to the system. Moreover, the distance the oil passes, while being heated in the thin gap, decreases. The maximum temperature for each case is plotted in **Fig. 7**. It drops with the increase of the pocket by approximately 20°C for both, 2000 rpm and 4000 rpm.

In all cases, in the area of the pocket, where the film is very thick, the shearing stress is small, or even negative due to oil flow irregularities. Downstream of the pocket (i.e. at the pad outlet side), the shear stress is larger for increased pocket cases than in the reference case. However, their values upstream of the pocket (at the inlet) are lower than the reference, almost reaching zero for Case 3. This is caused by the slow oil flow, since the outflow from the pocket is countered

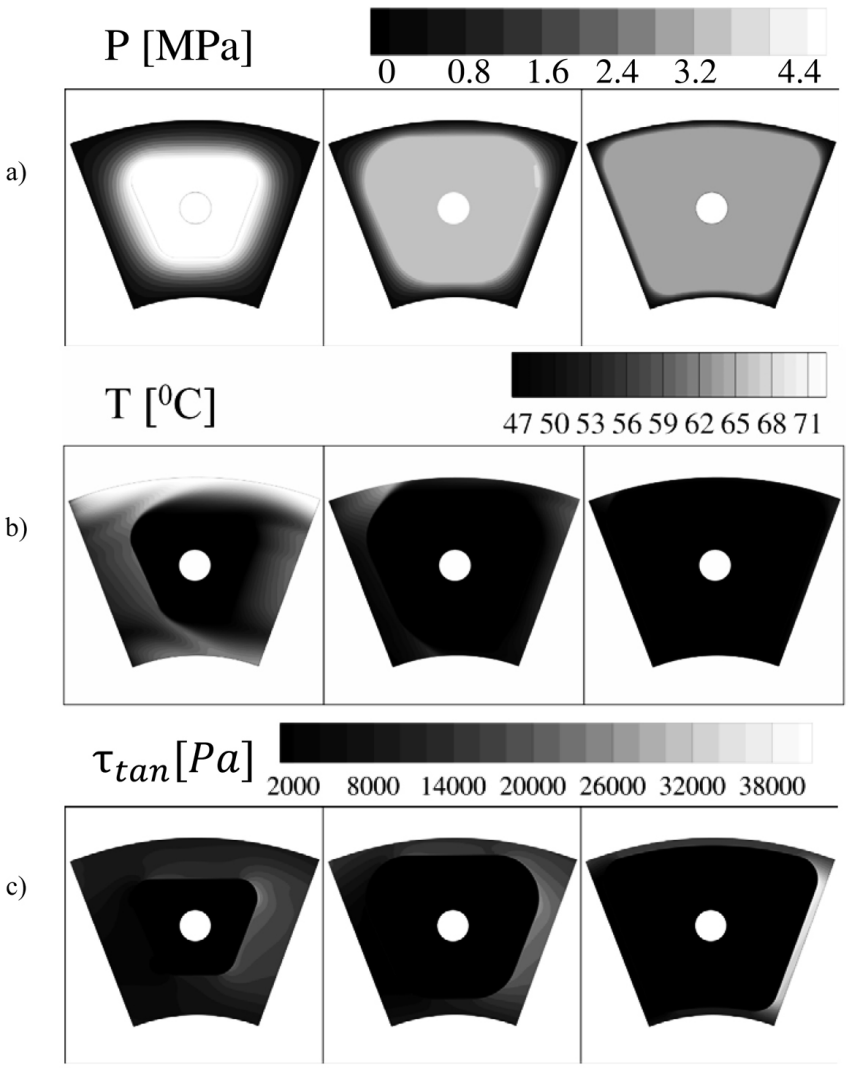

Fig. 5. The contours of pressure (a), temperature (b) and tangential shear stress (c) for hydrostatic bearing at 2000 rpm: left-hand column - Reference case, middle column – Case 1, right-hand column – Case 3 (clockwise collar rotation)

Rys. 5. Warstwice ciśnienia w filmie (a), temperatury (b) i naprężeń ścinających w łożysku hydrostatycznym przy 2000 obr./min: lewa kolumna – reference case, środkowa kolumna Case 1, prawa kolumna Case 3. Obrót tarczy zgodny z ruchem wskazówek zegara

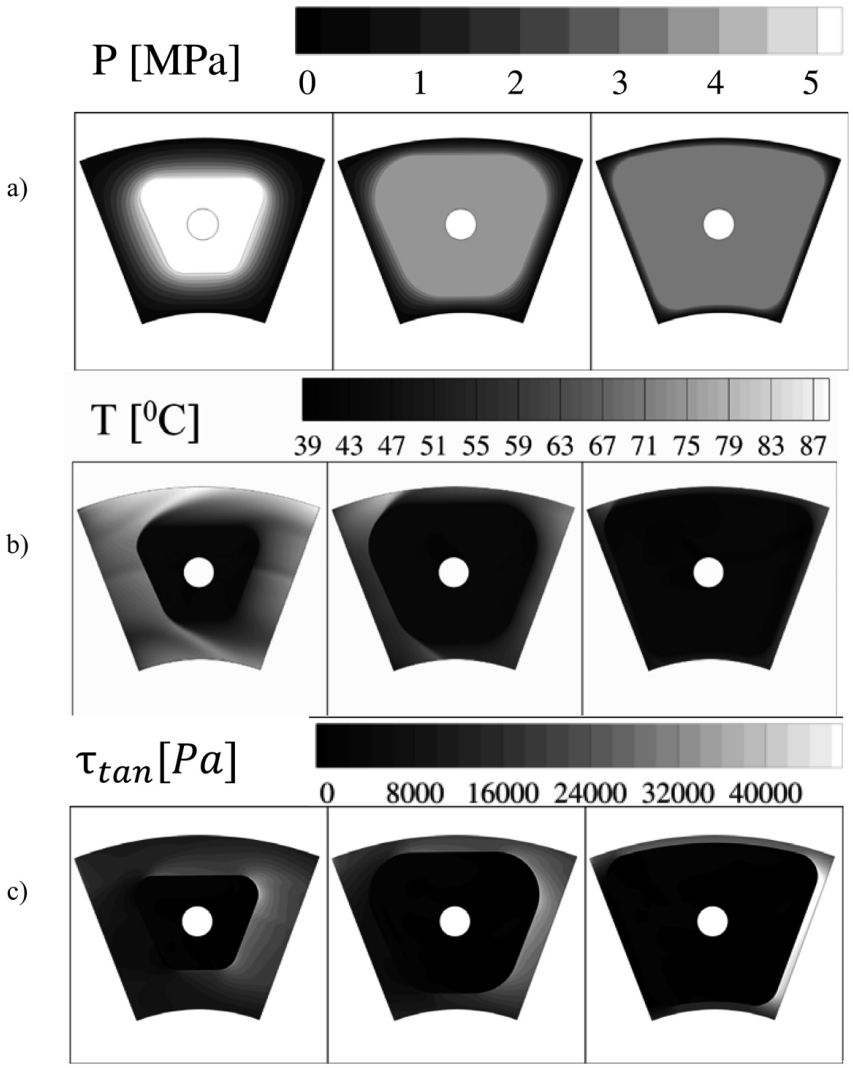

Fig. 6. The contours of pressure (a), temperature (b) and tangential shear stress (c) for hydrostatic at 4000 rpm: left-hand column – Reference case, middle column – Case 1, right-hand column – Case 3 (clockwise collar rotation)

Rys. 6. Warstwice ciśnienia w filmie (a), temperatury (b) i naprężeń ścinających w łożysku hydrostatycznym przy 4000 obr./min: lewa kolumna – Reference case, środkowa kolumna Case 1, prawa kolumna Case 3. Obrót tarczy zgodny z ruchem wskazówek zegara

by the flow caused by viscous pumping resulting from rotation of the collar.

Contour plots show the distribution of presented parameters over the surface of the whole pad, thus giving the possibility for qualitative comparison of parameters in both bearings, but it is not easy to compare the parameters quantitatively. That is why a set of graphs presenting selected parameters in selected cross sections was also prepared. Circumferential cross section at the mean radius and radial cross section through the middle of the pad, as shown in **Fig. 8**, were selected.

Circumferential pressure and temperature profiles for both bearings are shown in **Fig. 9**, and radial profiles are presented in **Fig. 10**. Pressure distributions show the decrease of the feeding pressure (and therefore, the pressure in the pocket). The lowering of the maximum temperature is also visible, especially on radial cross section, and the temperature on inner and outer radii drops significantly.

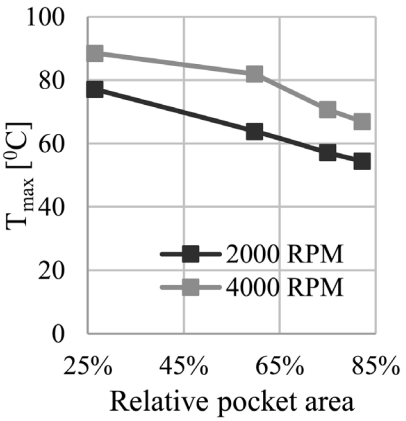

Fig. 7. Maximum film temperature for all studied cases of increasing pocket size and both rotational speeds

Rys. 7. Maksymalna temperatura w filmie smarowym dla różnych rozmiarów kieszeni i dla obu analizowanych prędkości obrotowych

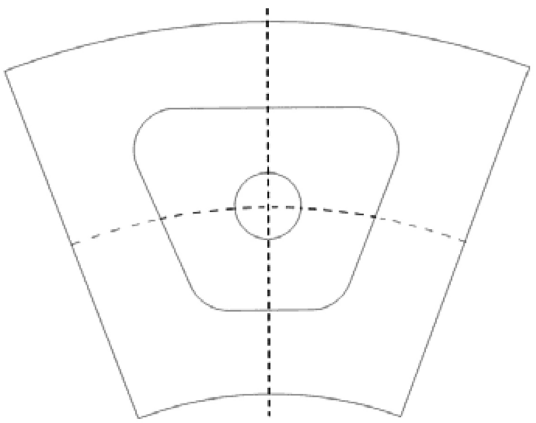

Fig. 8. Schematics of cutting surfaces for Fig. 9 and Fig. 10

Rys. 8. Schemat płaszczyzn przekroju dla wykresów z **Rys. 9** i **Rys. 10**

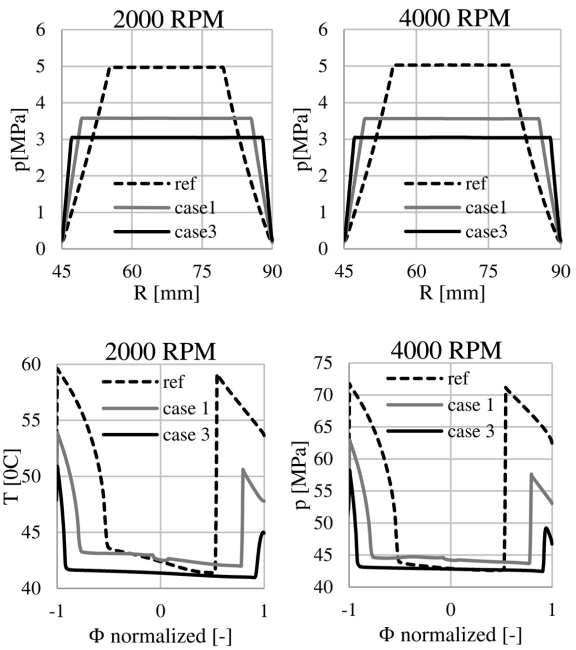

Fig. 9. Pressure and temperature of the bearing pad at 67.5 mm radius for hydrostatic bearing with various pocket sizes

Rys. 9. Przebieg ciśnienia w filmie i temperatury w obwodowym przekroju dla promienia 67,5 mm w łożysku hydrostatycznym z różną wielkością komory hydrostatycznej

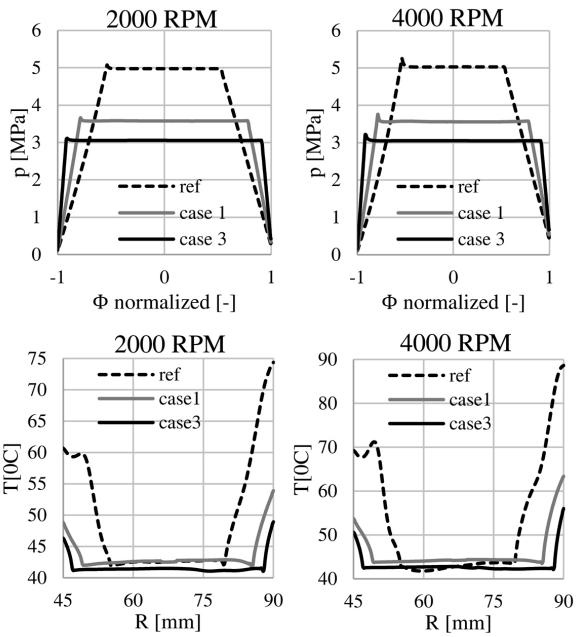

Fig. 10. Pressure and temperature of the bearing pad at angle 00 (middle of the pad) f for hydrostatic bearing with various pocket sizes

Rys. 10. Przebieg ciśnienia w filmie i temperatury w promieniowym przekroju dla kąta 0 w łożysku hydrostatycznym z różną wielkością komory hydrostatycznej

Losses in the bearings

In hydrostatic bearings, losses result from friction in the film and from pumping the oil, since its pressure is high and the flow is significant. Friction losses in the film were calculated by integrating the rotational shear stresses on the surface of the pad. Pumping losses are the product of volumetric flow rate and the pressure at the inlet. The results are collected in **Table 3** and **Table 4**, for 2000 rpm and 4000 rpm, respectively.

Table 3. Comparison of losses for various pocket area for 2000 rpm
Tabela 3. Porównanie strat dla różnych rozmiarów kieszeni dla 2000 obr./min

Pocket area [mm²]	579	1306	1637	1796
Pocket area/pad area	26%	60%	75%	82%
Inflow [l/min]	0.4	0.6	1.0	1.3
p_{inlet} [MPa]	5.0	3.6	3.2	3.1
Friction losses [kW]	2.1	1.5	1.2	1.0
Pumping losses [kW]	0.3	0.3	0.4	0.5
Total losses [kW]	2.3	1.8	1.6	1.5

Table 4. Comparison of losses for various pocket area for 4000 rpm
Tabela 4. Porównanie strat dla różnych rozmiarów kieszeni dla 4000 obr./min

Pocket area [mm²]	579	1306	1637	1796
Pocket area/pad area	26%	60%	75%	82%
Inflow [l/min]	0.8	1.3	1.9	2.6
p_{inlet} [MPa]	5.0	3.6	3.2	3.0
Friction losses [kW]	6.2	5.2	4.4	3.9
Pumping losses [kW]	0.6	0.6	0.8	1.0
Total losses [kW]	6.8	5.8	5.2	4.9

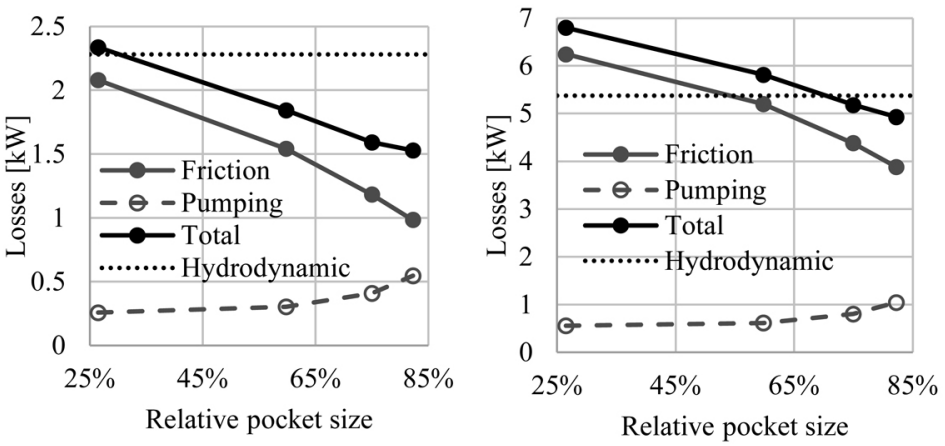

Fig. 11. Comparison of losses in both types of bearings at 2000 rpm (left-hand side) and 4000 rpm (right-hand side)
Rys. 11. Porównanie strat w obu typach łożysk przy prędkości obrotowej 2000 obr./min (po lewej) i 4000 obr./min (po prawej)

The losses are shown in **Fig. 11**, where they are also compared to the losses in the equivalent hydrodynamic bearing described in detail in the earlier paper [**L. 8**] and are equal to 2.28 kW and 5.37 kW for 2000 rpm and 4000 rpm, respectively. The graphs show that the friction losses decrease with the increase of the pocket size. This is caused by very low level of the shear stress in the pocket, which grows significantly in size. On the other hand, the pumping losses rise, due to increase oil flow. This is mitigated to some extent by the decrease of the feeding pressure, which can be lower, since it acts on larger area. Accordingly with the intentions of the research, the losses for pumping increase with the pocket increase, but they are still much lower than shearing losses in the film, especially at 2000 rpm. It means that the pocket size could have been even larger; howevr, for practical and design reasons, the pocket edge should have a reasonable thickness, so 2 mm were set as a limit. Interestingly, the feeding pressure tends to mean pressure resulting from the load. **Fig. 12** shows the feeding pressure (almost the same for 2000 rpm and 4000 rpm) and oil flow for all cases. The increase of the oil flow gets steeper for large pockets, since the edges of the pocket are thin and the short thin film gap generates lower resistance to flow. This causes a significant increase in pumping losses for large cavern.

Overall losses are a sum of friction (shearing) and pumping losses. For the first two pocket size increases, the rise of the pumping losses is easily mitigated by the drop in the friction losses, giving overall gain;

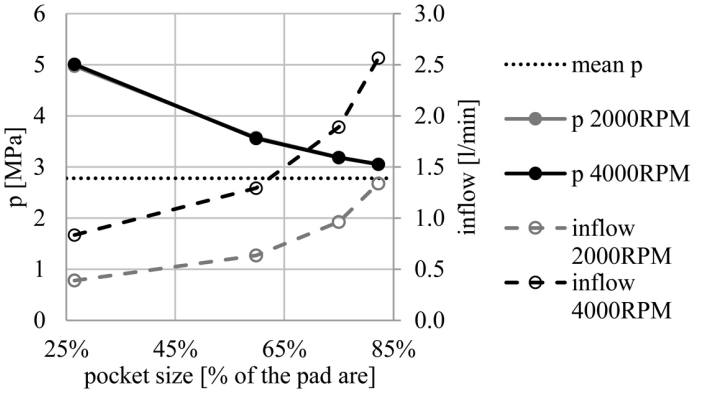

Fig. 12. Comparison of feeding pressure and oil flow in both types of bearings at 2000 rpm and 4000 rpm
Rys. 12. Porównanie ciśnienia zasilania i wydatku oleju w obu typach łożysk przy prędkości obrotowej 2000 obr./min i 4000 obr./min

however, for the largest gap, the effect is smaller, since the pumping losses increase drastically. For 2000 rpm, the decrease of losses from the reference case to the maximum pocket size is 35%, for 4000 rpm, it is 28%.

The results for the increased recess size are compared to the results of the hydrodynamic bearing. In case of 2000 rpm, even for the reference case the losses are similar. For slightly increased cavern size, the losses are already smaller than that for hydrodynamic bearing. For 4000 rpm case, the losses in the hydrostatic bearing get smaller than the hydrodynamic bearing for cavern area of around 70% of the pad area.

DISCUSSION OF RESULTS AND CONCLUSIONS

In the conclusions from the earlier paper [**L. 8**], the assumptions of calculations were discussed – the hydrostatic bearing was to carry the same axial load as the hydrodynamic bearing known from the literature. It was also decided to perform the calculations at approximately the same average film thickness, which results in much better safety of a hydrostatic bearing, because its minimum film thickness is larger (constant, approximately 30 μm for HS and minimum 9 μm for HD).

The earlier results showed moderate benefits at the rotational speed of 2000 rpm and no decrease of losses at 4000 rpm: At a lower rotational speed the difference was very small, approximately 3%, but at 4000 rpm, the power losses in a hydrostatic bearing were almost 20% larger than in a hydrodynamic bearing.

Looking at the results, it was concluded that further study should be directed into minimizing film shearing by increasing the size of the hydrostatic recess. The study presented in this paper showed that the defined direction of modifications was reasonable and brought the decrease of total losses by 0.8 kW, i.e. by 34% in case of 2000 rpm. The benefit was smaller at 4000 rpm and amounted to 0.5 kW, which is a decrease by 9%. In the best studied case with the largest recess size, its area comprised 82% of the total pad area, leaving only approximately 2 mm of the edge. The results show that a further increase of the pocket area could further decrease the total losses, but then the pocket edge would be very thin and difficult to machine and prone to damage during bearing handling.

ACKNOWLEDGEMENT

Calculations were carried out at Academic Computer Centre (TASK) in Gdańsk.

REFERENCES

1. Wasilczuk M.: Friction and Lubrication of Large Tilting-Pad Thrust Bearings. Lubricants 2015, 3, 164–180; doi:10.3390/lubricants3020164.
2. Abramovitz S.: Using Hydrostatic Bearings as “Lifts” in Hydroturbines. Hydro Rev. 2000, 19, pp. 38–47.
3. Dąbrowski L., Wasilczuk M.: Influence of Hydrostatic Pump Operation Period on Performance of a Thrust Bearing of a 125 MW Pump-turbine. Mec. Ind. 2004, 5, 3–9.

4. Dąbrowski L., Wasilczuk M.: Hydrostatic lift used in a steady state operation of a water turbine thrust bearing, Nordtrib 2006.
5. Ettles C.M.M., Seyler J., Bottenschein M.: Some effects of start-up and shut-down on thrust bearing assemblies in hydro-generators. Transactions of the ASME, Journal of Tribology, Vol. 125 (2003), p. 824–832.
6. Wasilczuk M., Wodtke M., Dąbrowski L.: Field Tests on Hydrodynamic and Hybrid Operation of a Bidirectional Thrust Bearing of a Pump-Turbine. Lubricants 2017, 5(4), 48; https://doi.org/10.3390/lubricants5040048.
7. Rippel H.: Projektirowanije gidrostaticzeskich podszipnikow (Design of hydrostatic bearings—In Russian translated from English). Izdatielstwo Maszinostrojenie , Moscow, Soviet Union, 1967, p. 16.
8. Wasilczuk F., Wasilczuk M., Wodtke M.: Prospects of Decreasing Power Losses in a Hydrostatic Thrust Bearing , TRIBOLOGIA, 4/2017, p. 91–96.
9. Wasilczuk M., Wodtke M., Braun W.: Centrally Pivoted Tilting Pad Thrust Bearing with Carbon-Based Coated Collar–Experimental Results of Low- and Medium-Speed Operation. Tribology Transactions, vol. 58 (Nr 5), 2015, s. 882–893.
10. Menter F.R.: Two-Equation Eddy-Viscosity Turbulence Models for Engineering Applications. AIAA Journal. 32(8). 1598–1605. August 1994.
11. Wodtke M., Olszewski A., Wasilczuk M.: Application of the fluid-structure interaction technique for the analysis of hydrodynamic lubrication problems. Proc IMechE, Part J: Journal of Engineering Tribology, 2013, vol. 227 (8), s. 888–897.